Ref. Ares(2021)7663151 - 11/12/2021

VirtualBrainCloud

Personalized Recommendations for Neurodegenerative Disease

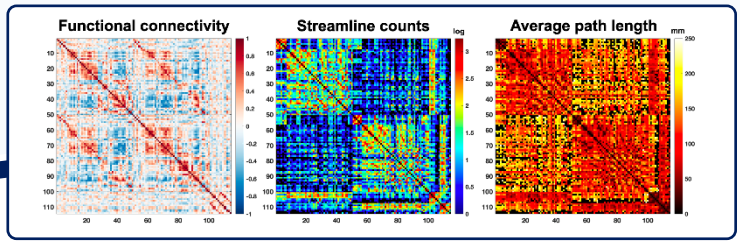

Public deliverable report

D3.2: Most appropriate RS-processing pipelines for TVB modelling finished

Date	November 2021
Authors	Institute of Neuroscience and Medicine (INM-7; Brain and Behaviour) Forschungszentrum Jülich: Kyesam Jung, Shufei Zhang, Oleksandr V. Popovych, Simon B. Eickhoff
Dissemination level	**public**
Website	www.VirtualBrainCloud-2020.eu

This project has received funding from the **European Union´s Horizon 2020** research and innovation programme under **grant agreement No 826421**

Table of content

1. Introduction 3
2. Partners involved 4
3. Description of work performed 4
4. Results 5
   4.1. Pipeline structure 5
   4.2. Pipeline performance 6
   4.3. Surface-based parcellation 10
   4.4. Model simulations 11
5. Conclusion, next steps 12
6. References 13

1. Introduction

Successful analysis of the neuroimaging data strongly relies on the data quality, where the appropriately selected and performed steps of the data (pre-)processing, cleaning and signal extraction play a crucial role (Ciric *et al.*, 2017; Maier-Hein *et al.*, 2017; Botvinik-Nezer *et al.*, 2020). The processing of the data from magnetic resonance imaging (MRI) is a complex procedure, involves many steps and approaches, and numerous software tools exist for this task (Soares et al. 2013; Schirner et al. 2015, 2021; Esteban et al. 2019). The current deliverable of the VirtualBrainCloud project also contributes to this field and presents a pipeline for the processing of MRI data, which is primarily designed for calculation of the structural and functional brain connectivities. The latter are used for derivation and validation of the data-driven whole-brain dynamical models (Ghosh *et al.*, 2008; Honey *et al.*, 2009) that are intensively investigated in the framework of the VirtualBrainCloud project. The structural connectivity (SC) calculated from the diffusion-weighted MRI (dwMRI) can be used to approximate the anatomical axonal connections in the brain and defines the underlying network of the models. The functional connectivity (FC) reflects the collective activity in the brain network, i.e., the extent of synchronization between network nodes and can be used for the model validation (fitting) against empirical data (Ghosh *et al.*, 2008; Honey *et al.*, 2009; Popovych *et al.*, 2019). At this, the model parameters are optimized in order to obtain the best correspondence between empirical and simulated FC.

The validated models can be applied for various purposes including modeling and investigation of the clinical data, study of the mechanisms underlying neurobiological phenomena and neuronal disorders, distinguishing between healthy subjects and clinical patients, and suggesting an approach for hypothesis testing *in silico* (Jirsa *et al.*, 2017; Zimmermann *et al.*, 2018; Deco *et al.*, 2019; Popovych *et al.*, 2019). The model derivation and validation procedure may however follow different approaches depending on the level of model personalization. In particular, the modeling may take place either at the group level by considering SC matrices averaged over the entire subject cohort, or at the individual level by considering personalized models based on individual SC for every subjects separately (Deco *et al.*, 2019; Popovych *et al.*, 2021). Further enhancement of the model personalization may be achieved by adding into the model additional region-specific and potentially personalized subject-specific features extracted from the empirical data such as frequencies and amplitudes of the empirical time series, excitation-inhibition balance or distribution of the neuronal receptors (Deco *et al.*, 2019; Demirtas *et al.*, 2019; Kringelbach *et al.*, 2020; Domhof *et al.*, 2021; Jung, Eickhoff and Popovych, 2021; Popovych *et al.*, 2021). Model personalization can potentially contribute to accurate modeling of brain activity, capture subject-specific differences in both structure and dynamics and reflect brain changes related to disease states such as epilepsy or Alzheimer's disease (Jirsa *et al.*, 2017; Bansal, Nakuci and Muldoon, 2018; Zimmermann *et al.*, 2018). This can be of relevance in the framework of personalized approaches in medicine (Falcon, Jirsa and Solodkin, 2016). It is however unclear how the desired personalization of the whole-brain dynamical models can be established.

This deliverable contributes to the discussed topic, where the data and model personalization can be incorporated into the analysis and modeling workflow already at the level of data processing and signal extraction. We thus extended, improved and finalized the pipeline previously developed and reported in the Deliverable D3.1 "Initial version of full-scope containerized pipeline developed" (Jung *et al.*, 2020) to provide an individualized approach for the neuroimaging data processing. In particular, the new version of the pipeline can provide the whole-brain tractography and SC calculated from dwMRI, and

blood oxygen level-dependent (BOLD) signals and FC inferred from the resting-state functional MRI (fMRI) in the corresponding native spaces. We can thus avoid the complex nonlinear transformation of the individual brains to the standard MNI152 space (Evans *et al.*, 2012), which involves unnecessary data deformation. The later brain normalization is especially harmful for the brains that notably deviate from the template brain, as, for example, in the case of brains with atrophies or injuries, which can frequently be observed in clinical data and for older subjects. Furthermore, brain normalization to the standard template may to some extent suppress the brain inter-individual variability that can be an important feature for differentiation between individual subjects in health and disease. With this pipeline we may investigate how the model personalization at the stages of the data processing and its modeling can influence the model properties and its outcome.

2. Partners involved

This deliverable was prepared by the Institute of Neuroscience and Medicine (Brain and Behaviour, INM-7) from the Forschungszentrum Jülich (FZJ). The computational resources were granted through JARA on the supercomputer JURECA (Jülich Supercomputing Centre, 2018) at Jülich Supercomputing Centre, Forschungszentrum Jülich.

3. Description of work performed

The developed pipeline is an open-source collection of shell scripts based on several well-established and freely available software packages that are widely used in the neuroimaging community. It has a modular structure, where every module can be executed independently of the others provided that the corresponding input data is available. This contributes to the flexibility of pipeline application, in particular, as related to selection of parameters and algorithms of the data processing, cleaning and signal extraction, which is important for the model-based investigation of brain dynamics. The pipeline was tested on different hardware and software environments ranging from single-core desktops and local clusters to supercomputers (Jülich Supercomputing Centre, 2018), where the pipeline was optimized for parallel processing of several subjects on multi-thread computational nodes. Furthermore, the results of the data processing by our personalized pipeline were compared to the standard approach involving brain normalization to the MNI152 space as well as to other well-established pipelines of the neuroimaging data processing.

One of the motivations to develop a personalized pipeline is illustrated in Fig.1, where an example of the image pre-processing of a brain with atrophy is shown. The considered brain image exhibits an atrophy in the left hemisphere (Fig.1, lower plot), and the nonlinear transformation from the standard MNI152 space to the native T1-weighted (T1w) space resulted in a strong deformation of the left side of the head (compare colored and gray-scaled images in Fig. 1, upper plot). The normalization procedure is apparently unable to account for such an enhanced deviation from the template brain, which is supposed to have further impairments on the quality of the consecutive signal extraction, its analysis and modeling.

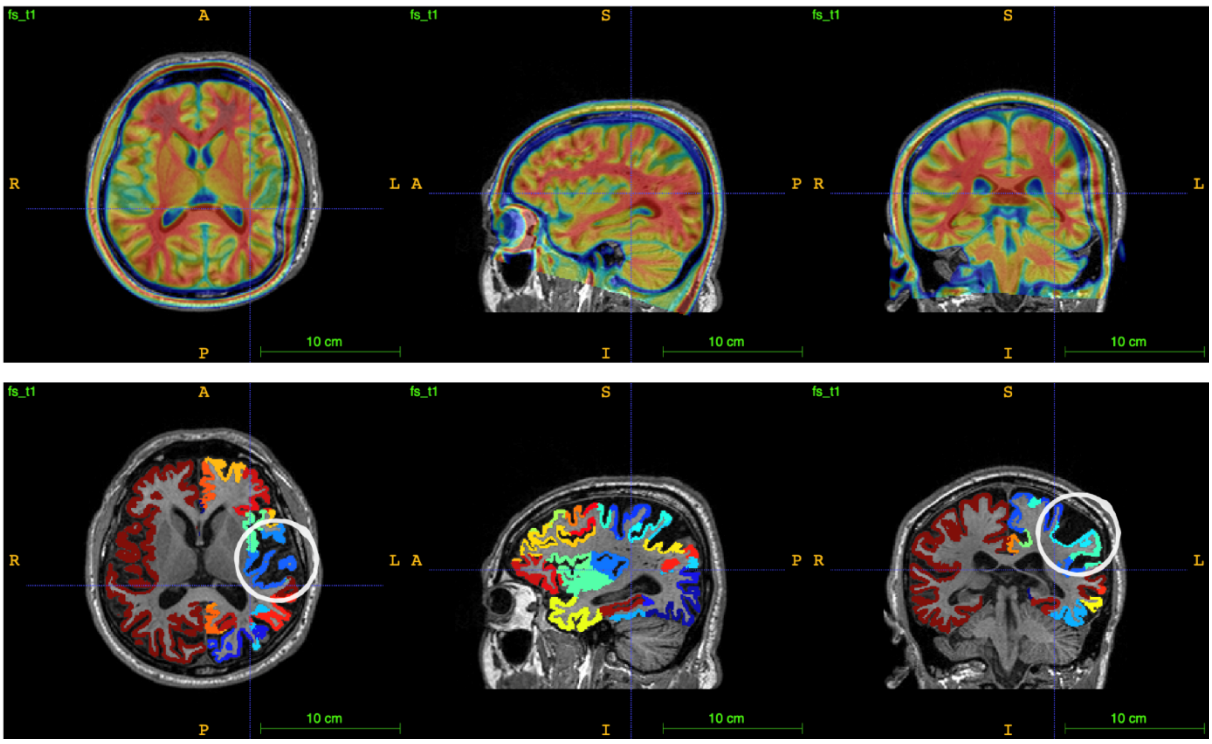

Figure 1: Upper plot: Example of the nonlinear image transformation from the MNI152 T1-weighted (T1w) template (RGB colors) to T1w image in the native space (gray colors as the background image). Lower plot: Example of the brain parcellation (colored regions) based on the classifier of the Schaefer atlas (Schaefer *et al.*, 2018) with 100 parcels in the native T1-w image space (the same gray-scale background as in the upper plot). The white circles indicate brain areas of the atrophy.

To resolve this problem we suggest to process the brain images completely in their native spaces without any transformation to the standard space. The main component of such a procedure is an appropriate brain parcellation that can be used to compare the extracted signals and connectivities across individual subjects. Such a personalized parcellation can be performed with surface-based approach to parcel cortical brain areas (Desikan et al., 2006; Fischl et al., 2004). For our goals, it uses cortical geometric information in the native space and does not require any nonlinear deformation process from the standard to native spaces to bring parcellation information. Subsequently, the parcellation via the surface-based method appears to be accurate in the native space as illustrated in Fig. 1 (lower plot) for the same subject, where the normalization procedure failed [Fig. 1, upper plot]. We thus included the discussed surface-based personalized parcellation in our pipeline to enable the data processing and signal extraction in the native spaces.

4. Results

4.1. Pipeline structure

The structure of the developed pipeline is schematically illustrated in Fig. 2. It includes the pre-processing of T1w images, dwMRI and fMRI data as well as brain parcellation in the native spaces and extraction of the whole-brain tractography, SC, BOLD signals and FC. In the pipeline scripts some functions of several third-party software packages were used including FSL (Jenkinson et al., 2012), MRtrix (Tournier et al., 2019), ANTs (Tustison et al., 2014), FreeSurfer (Dale, Fischl and Sereno, 1999),

AFNI (Cox, 1996) and Connectome Workbench (Glasser et al., 2013). Further details on the performed main steps of the data processing, utilized software packages and executed functions of the pipelines for dwMRI and fMRI data can be found in the previous deliverable D3.1 of 2020 (Jung et al., 2020) The difference consists in a new option to extract the signals and calculate the structural and functional connectomes in the native spaces. This option can replace the image normalization to MNI152 space, which can however also be included in the setup of the pipeline as an optional additional step. The pre-processing modules 1 and 5 can now be completed by co-registration between T1w and diffusion weighted image (DWI) for dwMRI pipeline and between T1w and echo-planar imaging (EPI) for fMRI pipeline and then by transforming the parcellation labeling to the corresponding native images. This will be sufficient for the atlas-based extraction of SC and BOLD signals (and FC) from the pre-processed imaging data in the native spaces.

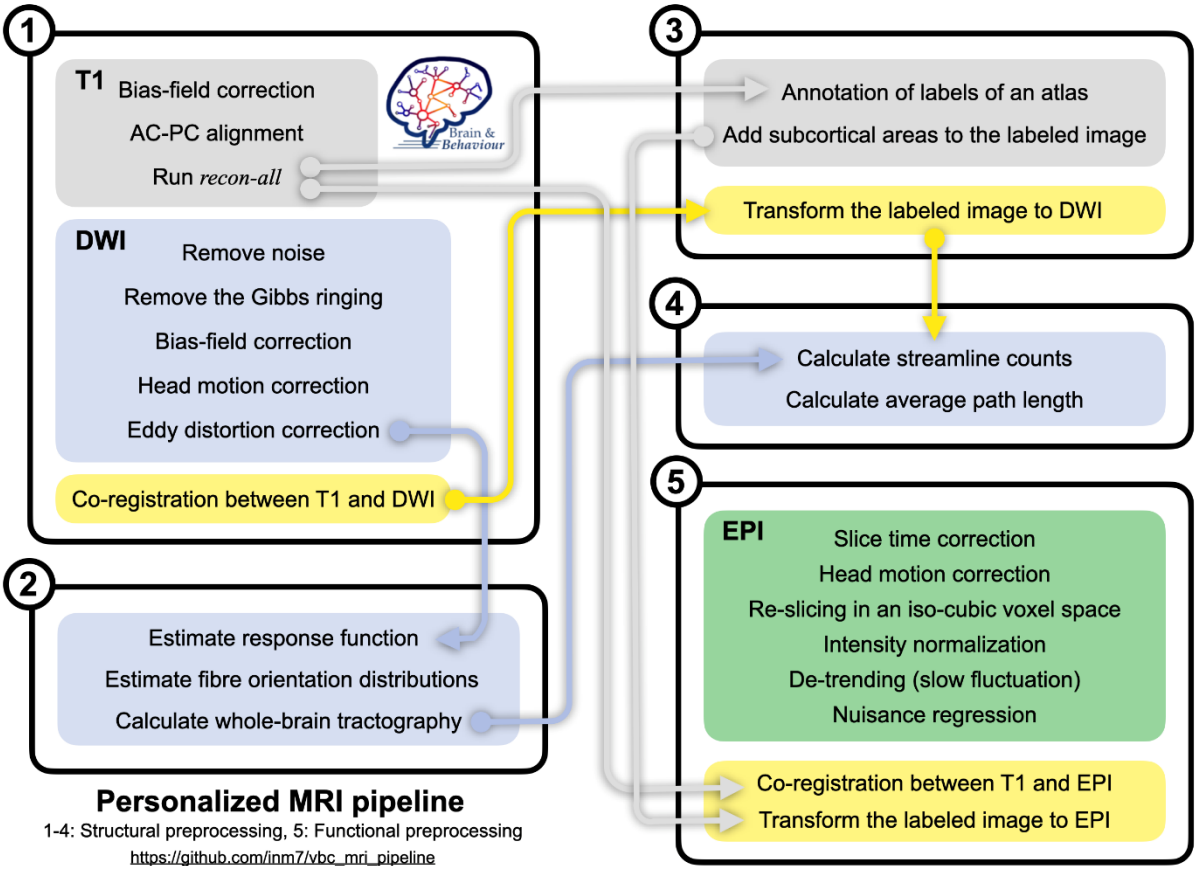

Figure 2: Schematic illustration of the pipeline workflow for personalized data processing and signal extraction. The independent modules are encircled in enumerated rectangular blocks with performed data processing steps indicated, where the operations shadowed in color are used to process T1w images (gray), dwMRI data (light blue) and fMRI data (green). The updated parts of the pipelines necessary for parcellations in the native spaces are indicated in yellow. The arrows depict the interdependence (required input) between the modules.

4.2. Pipeline performance

The discussed pipeline was applied to process the raw neuroimaging data, parcellate the brain according to a given atlas in the native space and extract the structural and functional connectomes. An example of the pipeline results is illustrated in Fig. 3. As follows, the parcellation accurately reflects the folding structure of the cortex and appropriately splits the gray matter into the parcellated brain regions [Fig.

3, upper plot, see also Fig. 1]. The corresponding personalized (i.e., calculated in the native spaces) functional and structural connectomes also illustrated in Fig. 3 (lower plots), which represent well the hemispheric separation of the functional and structural connectivity and the included subcortical areas corresponding the brain regions with indices larger than 100 [Fig. 3].

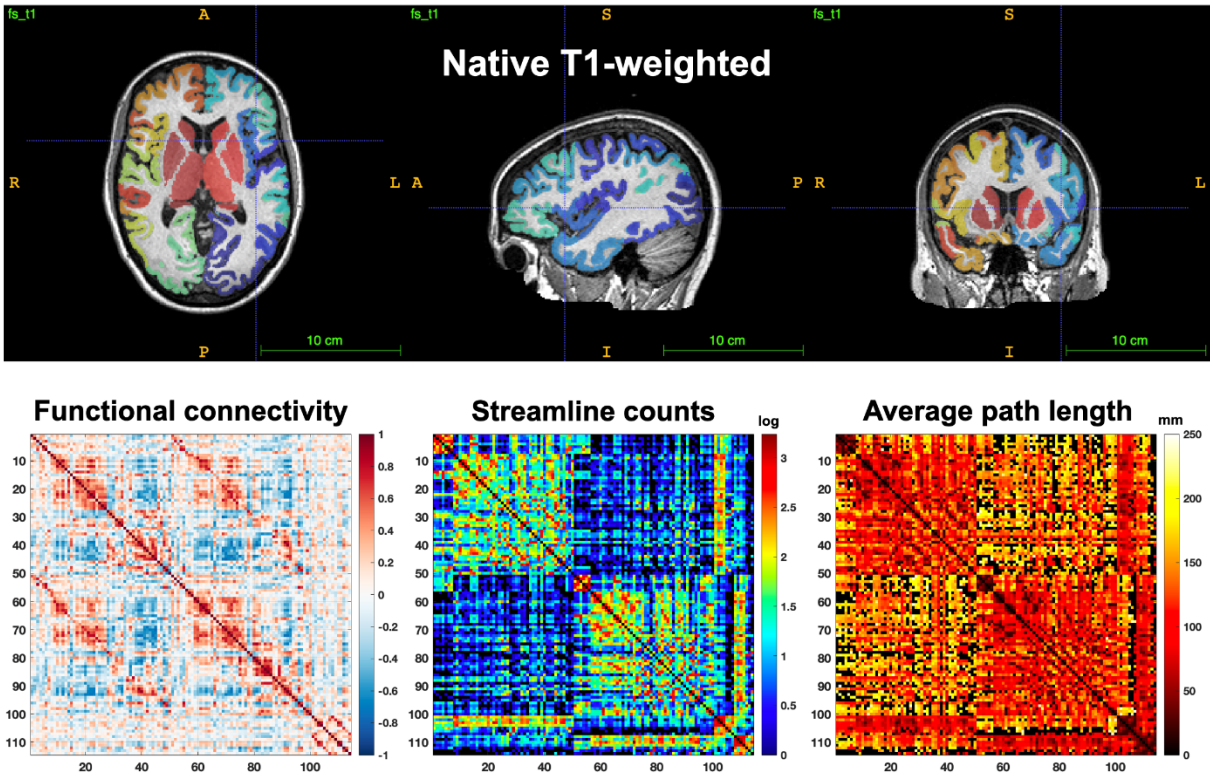

Figure 3: Examples of the pipeline results of the brain parcellation in the native space (upper plot) and extraction of the personalized (native) functional and structural connectomes (lower plots) for the Schaefer atlas (Schaefer *et al.*, 2018) with 100 brain regions. The connectomes are represented by the resting-state FC, and the matrices of the streamline counts and averaged streamline path length between the brain parcels as indicated in the plots.

The structural connectomes extracted by the personalized pipeline can be compared with those calculated for the volumetric brain atlases transformed from the standard MNI152 space [Fig. 4]. The similarity is high for the streamline count matrices practically for all considered total numbers of the streamlines of the whole-brain tractography [Fig. 4, upper plot]. We can however note somewhat reduced agreement for smaller tractography density (number of streamlines). The agreement is lower for PL matrices [Fig. 4, lower plot], but the sensitivity of the PL matrices is a known property that can also be observed for repetitive recalculations of PL matrices by the same or different pipelines (Jung et al., 2020). The PL-similarity reported in Fig. 4 is approximately in the same range observed for such recalculations. We thus conclude that the personalized pipeline effectively delivers the structural connectomes that are close to those calculated by the established approach via a transformation of the brain atlases from the standard MNI152 space.

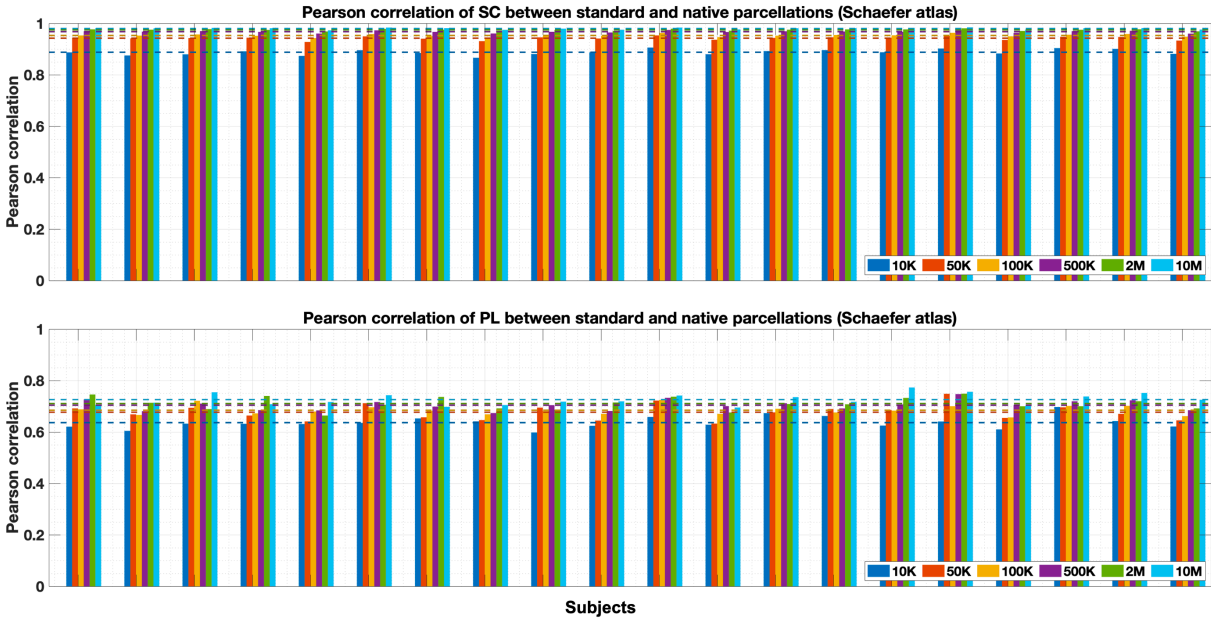

Figure 4. Similarity as given by Pearson correlation between structural connectomes calculated either after transformation of the atlas from the standard MNI152 space or by the personalized parcellation in the native space. The parcellation was performed according to the Schaefer atlas with 100 brain regions, for the several tractography densities as given by the total number of streamlines of the whole-brain tractography indicated in the legend, and for 20 subjects. The upper and lower plots depict the similarities for the streamline count (SC) and PL matrices, respectively. The dashed color lines indicate mean values of each tractography density conditions (in different colors).

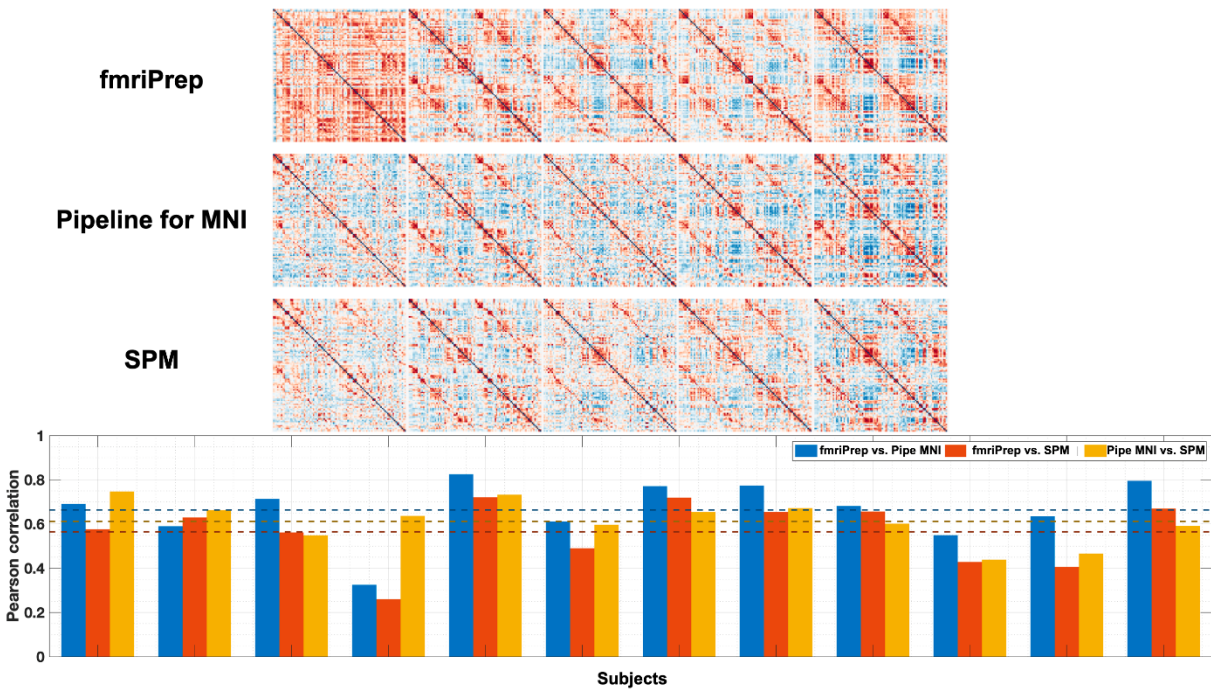

Figure 5: Comparing functional connectomes for several pipelines (the current pipeline, fMRIPrep and SPM) when FC was calculated from BOLD signals extracted in the standard MNI152 space. Examples of FC matrices for the Schaefer atlas with 100 parcels are illustrated for a few subjects (started from subject #4) in the upper plots with the used pipeline indicated. The similarity (Pearson correlation) between FC of different pipelines is shown in the

lower plot for several subjects, where the corresponding pairwise comparisons between the pipelines are indicated in the legend.

We also evaluate and compare the performance of our pipeline for processing of the resting-state fMRI data with a few other widely-used neuroimaging pipelines, in particular, with SPM (Friston, 2008) and fMRIPrep (Esteban et al., 2019). A few examples of FC calculated by the considered pipelines in the standard MNI152 space are illustrated in Fig. 5 (upper plots). Our pipeline in MNI152 space produces FC similar to those of the other pipelines. From the three pairwise comparisons, our pipeline appears to be closest to fMRIPrep and then to SPM, see Fig. 5 (lower plots). The outputs of the two well-established pipelines, fMRIPrep and SPM are the most distant to each other. These results demonstrate that our pipeline performs well in MNI152 space and its output (FC) is similar to other pipelines.

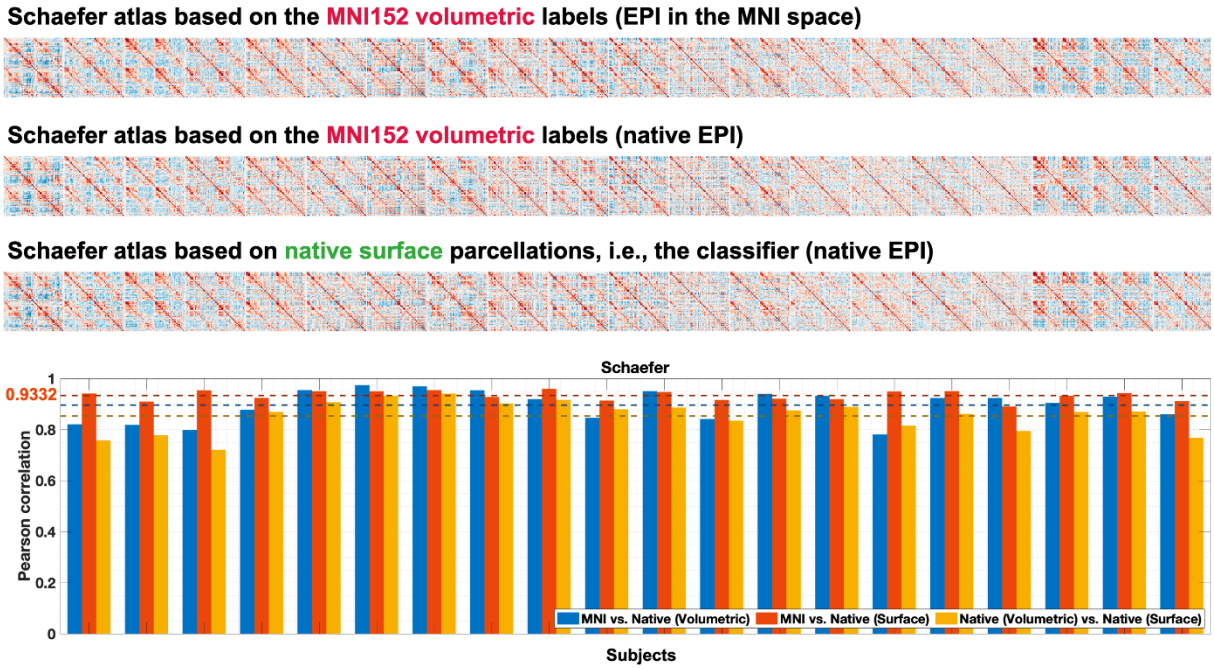

Figure 6: Performance of the developed pipeline for processing of the resting-state fMRI data the in the EPI native space as compared to the data processing in the MNI152 space and transformation between the spaces. Examples of the FC matrices for the Schaefer atlas with 100 parcels are shown in the upper plots for the case of volumetric parcellation in the standard MNI152 space (denoted as “EPI in MNI” or “MNI volumetric”), transformation of the volumetric atlas from the MNI152 space to the native EPI space (denoted as “native volumetric”), and for the surface-based parcellation only in the native space (denoted as “native surface”). The similarity (Pearson correlation) between FC matrices obtained for the considered cases is illustrated in the lower plot, where corresponding pairwise comparisons are indicated in the legend.

The performance of the developed personalized pipeline at the processing for the resting-state fMRI data in the native space can be illustrated by comparing FC matrices calculated in different spaces of the brain parcellations. We thus consider the brain parcellation by a volumetric atlas in MNI152 space (“MNI volumetric”), volumetric parcellation in the native space, where the atlas was transformed from MNI152 to the native space (“native volumetric”), and surface-based parcellation in the native space only (“native surface”). In all cases, the pipeline produces similar results as can be observed for the patterns of the functional connectomes [Fig. 6, upper plots], which is also confirmed by high Pearson correlations between FC matrices [Fig. 6, lower plot]. FCs obtained by personalized calculations (i.e., in

the "native surface" case) have connectivity patterns that are closest to those calculated in the standard MNI152 space [Fig. 6, lower plot, red bars] and then to those obtained after the transformation of volumetric atlas from MNI152 to native space. Based on the presented results we conclude that the personalized processing of the resting-state fMRI data and connectivity calculation in the native space are stable and do not strongly deviate from the results obtained by an established approach in the standard MNI152 space.

#subjects (threads)	structural pipeline		functional pipeline	
	time(min)	speedup	time(min)	speedup
4 (64)	361.1	1.0	253.7	1.0
8 (32)	359.0	2.0	262.6	2.1
16 (16)	371.5	3.9	268.0	4.2
32 (8)	411.9	7.0	295.0	8.1
64 (4)	**480.2**	**12.0**	**365.5**	**15.9**

Table 1: Speedup values of the scaling illustrated in Fig. 7. The number of threads assigned to each subject are indicated in parentheses.

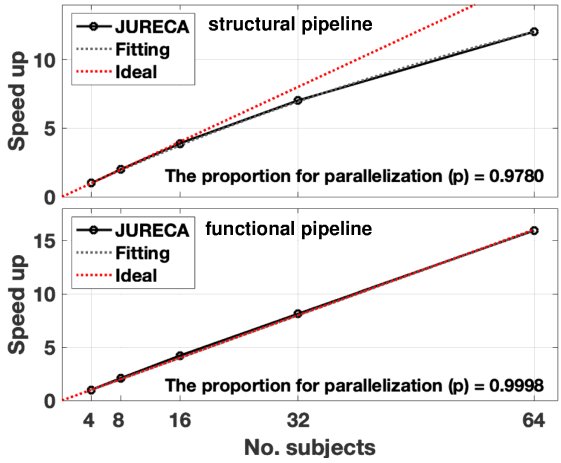

Figure 7: Scaling behavior of the structural (upper plot) and functional (lower plot) pipelines on one node of CPU partition of JURECA-DC by parallel processing of several subjects.

The pipeline was tested and optimized for execution on the high-performance clusters in order to process large subject cohorts. The performance and the scaling of the pipelines on JURECA-DC CPU nodes (Jülich Supercomputing Centre, 2018) at Jülich Supercomputing Centre, Forschungszentrum Jülich were evaluated and illustrated in Fig. 7 and Table 1, where the parallelized part p of the code according to Amdahl's law is also indicated. The optimal configurations of both (structural and functional) pipelines is realized when 64 subjects were simultaneously processed on one CPU node with 256 threads (4 threads per task/subject). The number of subjects was mostly limited by the memory usage, where approximately 8GB were at least necessary to process one subject, i.e., 64 subjects fit to 512GB of the node memory.

4.3. Surface-based parcellation

In the case when a given atlas of interest does not provide a classifier necessary to parcel cortical areas on the surface in the native T1w space, we can also train the corresponding classifier. This can be accomplished for a given subject cohort when a volumetric parcellation is applied to individual brains in the standard MNI152 space, which then are used to create a classifier. For example, Fig. 8 illustrates the process of creating a classifier based on transformed volumetric images from the MNI153 space for the Harvard-Oxford atlas that is distributed in the volumetric format in the standard space. Based on individual volumetric labeled images, the labels can be projected on the vertices of cortical surfaces [Fig. 8A]. The vertices of individual cortical surfaces can be matched as the same geometric locations across subjects. Accordingly, the labels on the vertices can be summarized to have the most frequent label as representative ones. Subsequently, we have the representative annotation on the vertices based on the used subject sample. The annotation file is used to generate a classifier.

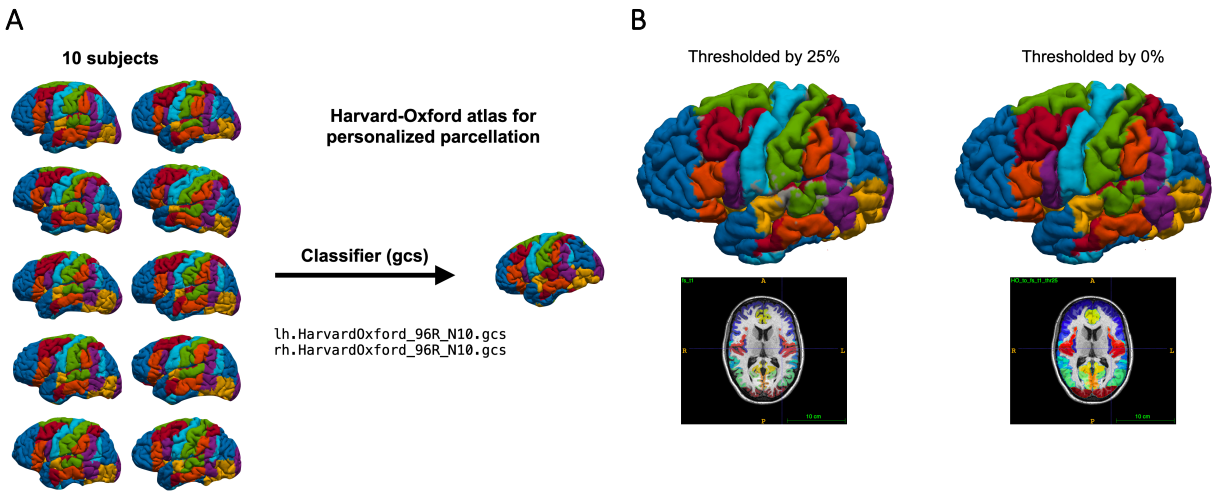

Figure 8: Calculation of the atlas classifier necessary for surface-based brain parcellation in the native space. (**A**) Schematic illustration that volumetric parcellations in the standard space of several subjects can be used to build a classifier. (**B**) Examples of the brain parcellations in the native space obtained by training the classifier from the volumetric Harvard-Oxford atlas with 0% (right plots) and 25% (left plots) maximal probability thresholds.

Following the above procedure, we created the classifiers of the Harvard-Oxford atlas for each hemisphere, see Fig. 8B, where annotation examples corresponding to different levels of 0% or 25% of the maximal probability threshold were used for the Harvard-Oxford atlas. In the case of 25% thresholding, one can observe some empty vertices (gray color in Fig. 8B) due to compact cortical volumes on the MNI152 space, which can give relatively thinner cortical gray matter caused by some strong deformation during inverse-normalization. In contrast, the 0% thresholding gives relatively large region volumes which can cover much more vertices and the empty vertices are practically absent. Therefore, we used 0% thresholding to create the classifiers of the Harvard-Oxford atlas. Our pipeline includes the corresponding scripts for the training of the classifiers for a volumetric atlas in the standard space and for a given cohort of subjects.

4.4. Model simulations

Empirical structural connectomes extracted by the discussed personalized pipeline for a given brain parcellation were used to derive the model network. The normalized streamline counts between any two brain regions were considered as the corresponding coupling strength between the respective network nodes, and the average path lengths were used to calculate the time delay of signal propagation between the nodes. Equipping the individual nodes by local dynamics allow then to generate simulated BOLD signals and thus calculate a simulate FC. The latter will be compared with empirical FC again calculated by the personalized pipeline, and the model parameters are optimized in order to obtain the strongest correspondence between the simulated and empirical data [Fig. 9, upper left]. This constitutes the model validation. Such optimal model parameters of the largest goodness-of-fit values as given by Pearson correlation between simulated and empirical FC are illustrated in Fig. 9 (lower left). Examples of the empirical and simulated BOLD and FC for the validated model are illustrated in Fig. 9 (middle and right columns). One observes that the simulated data can relatively well correspond to the empirical data, and the optimal parameters are in a biologically feasible range, e.g., the global

time delay in coupling. Based on the obtained results we conclude that the pesonalized pipeline is ready for application, and the extracted data, e.g., connectomes calculated in the native spaces can be used for personalized modeling of the resting-state brain activity.

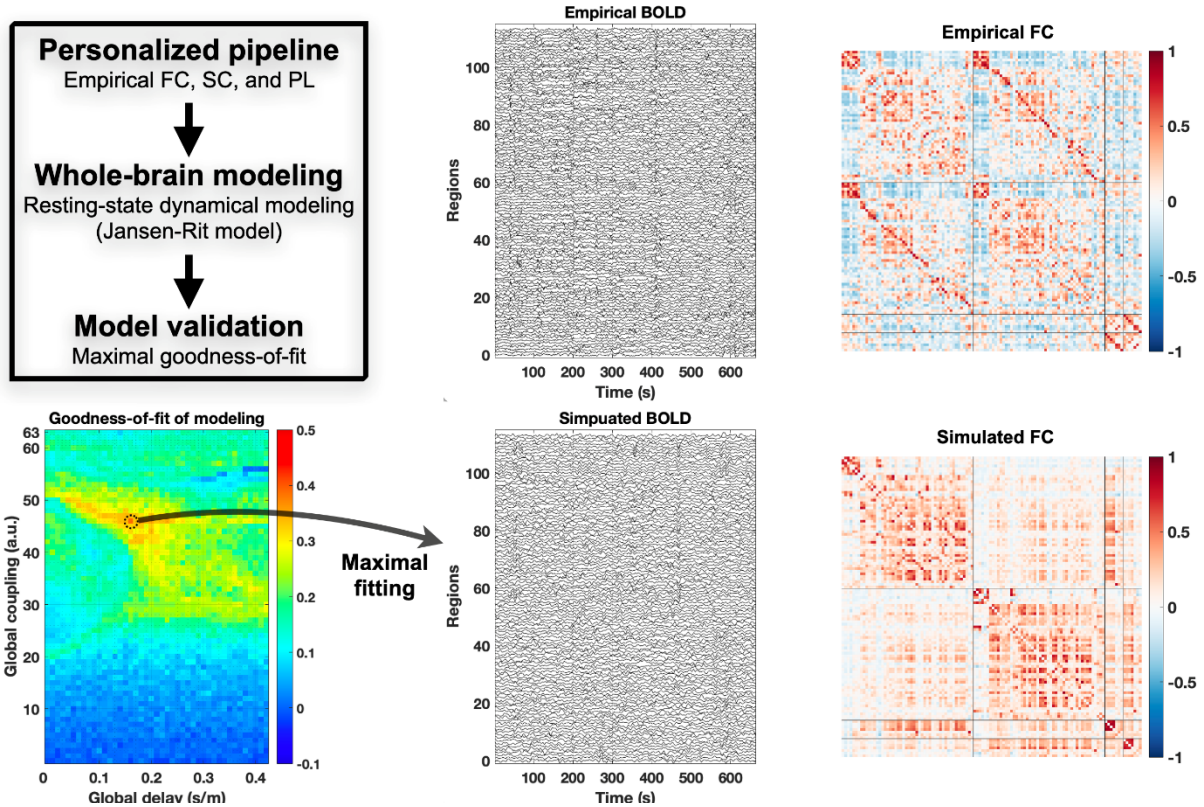

Figure 9: Example of the whole-brain modeling workflow based on the personalized data processing and signal extraction. The connectivity matrices SC, PL and FC are extracted from the empirical neuroimaging data and used for model derivation and validation. Lower left plot: The optimal model parameters of the maximal similarity between empirical and simulated FC. Middle column: examples of the empirical and simulated BOLD signals for the optimal model parameters. Right column: Examples of the empirical and simulated FC matrices of their best fit to each other.

5. Conclusion, next steps

We developed the next version of the pipeline that can be used for pre-processing of the neuroimaging data in the native spaces of the brain images without involving a complex nonlinear transformation to the standard MNI152 space. This is supposed to reduce the complex manipulation with data and facilitate the investigation of the inter-individual differences. The normalization of the brain images to the standard space may also fail, especially, for the clinical data or for older population, where the brain atrophy or other reasons may strongly deviate the brain images from the standard template. We showed that the developed pipeline performs relatively well when comparing to other widely used pipelines as well as to the standard approach designed to involve the data normalization to the standard space and brain parcellation in the MNI152 space. An essential condition for such a personalized data processing, analysis and modeling is a brain parcellation in the native space that can be realized via a surface-based brain parcellation. The presented pipeline includes several such parcellations known from the literature. Moreover we also developed a corresponding approach and included the respective script in the pipeline for training a classifier for personalized brain parcellation if a volumetric atlas

defined in the standard MNI152 space is available. The developed pipeline was also successfully tested for the whole-brain modeling of the resting-state brain activity. The pipeline is available in dedicated projects on GitHub. The repositories contain all code and documentation necessary to apply the pipeline to the pre-processing the neuroimaging data and extraction of the signals including the whole-brain tractography, SC, BOLD signals and FC:

https://jugit.fz-juelich.de/inm7/public/vbc-mri-pipeline

The next steps may include the investigation of the interindividual differences in health and disease and therefore involving clinical data for processing with developed personalized pipeline. The obtained empirical data, e.g., structural and functional connectomes can be used for personalized model-based investigation of the resting-state brain and its connection to behavior. The modeling results can be related to the phenotypical data of the patients and healthy controls in order to better understand the differences between diseased and healthy brain states, differentiation between them and, ultimately, suggest and test possible therapeutic intervention.

6. References

Bansal, K., Nakuci, J. and Muldoon, S.F. (2018) 'Personalized brain network models for assessing structure-function relationships', Curr. Opin. Neurobiol., 52, pp. 42–47. doi:10.1016/j.conb.2018.04.014.

Botvinik-Nezer, R. et al. (2020) 'Variability in the analysis of a single neuroimaging dataset by many teams', Nature, 582(7810), pp. 84–88.

Ciric, R. et al. (2017) 'Benchmarking of participant-level confound regression strategies for the control of motion artifact in studies of functional connectivity', Neuroimage, 154, pp. 174–187. doi:10.1016/j.neuroimage.2017.03.020.

Cox, R.W. (1996) 'AFNI: Software for analysis and visualization of functional magnetic resonance neuroimages', Comput. Biomed. Res., 29(3), pp. 162–173. doi:10.1006/cbmr.1996.0014.

Dale, A.M., Fischl, B. and Sereno, M.I. (1999) 'Cortical surface-based analysis. I. Segmentation and surface reconstruction', Neuroimage, 9, pp. 179–194.

Deco, G. et al. (2019) 'Awakening: Predicting external stimulation to force transitions between different brain states', Proc. Natl. Acad. Sci. U. S. A., 116(36), pp. 18088–18097. doi:10.1073/pnas.1905534116.

Demirtas, M. et al. (2019) 'Hierarchical Heterogeneity across Human Cortex Shapes Large-Scale Neural Dynamics', Neuron, 101(6), pp. 1181–+. doi:10.1016/j.neuron.2019.01.017.

Desikan, R.S. et al. (2006) 'An automated labeling system for subdividing the human cerebral cortex on MRI scans into gyral based regions of interest', Neuroimage, 31(3), pp. 968–980. doi:10.1016/j.neuroimage.2006.01.021.

Domhof, J.W.M. et al. (2021) 'Parcellation-induced variation of empirical and simulated brain connectomes at group and subject levels', Network Neuroscience, 5(3), pp. 798–830. doi:10.1162/netn_a_00202.

Esteban, O. et al. (2019) 'fMRIPrep: a robust preprocessing pipeline for functional MRI', Nat. Methods, 16(1), pp. 111–+. doi:10.1038/s41592-018-0235-4.

Evans, A.C. et al. (2012) 'Brain templates and atlases', NeuroImage, 62(2), pp. 911–922. doi:https://doi.org/10.1016/j.neuroimage.2012.01.024.

Falcon, M.I., Jirsa, V. and Solodkin, A. (2016) 'A new neuroinformatics approach to personalized medicine in neurology: The Virtual Brain', Curr. Opin. Neurol., 29(4), pp. 429–436. doi:10.1097/WCO.0000000000000344.

Fischl, B. et al. (2004) 'Automatically Parcellating the Human Cerebral Cortex', Cereb. Cortex, 14(1), pp. 11–22. doi:10.1093/cercor/bhg087.

Fischl, B. (2012) 'FreeSurfer', NeuroImage, 62(2), pp. 774–781. doi:https://doi.org/10.1016/j.neuroimage.2012.01.021.

Friston, K. (2008) Statistical parametric mapping : the analysis of functional brain images. Amsterdam: Academic Press.

Ghosh, A. et al. (2008) 'Noise during Rest Enables the Exploration of the Brain's Dynamic Repertoire', PLoS Comput. Biol., 4(10), p. e1000196. doi:10.1371/journal.pcbi.1000196.

Glasser, M.F. et al. (2013) 'The minimal preprocessing pipelines for the Human Connectome Project', Neuroimage, 80, pp. 105–124. doi:10.1016/j.neuroimage.2013.04.127.

Honey, C.J. et al. (2009) 'Predicting human resting-state functional connectivity from structural connectivity', Proc. Natl. Acad. Sci. U. S. A., 106(6), pp. 2035–2040. doi:10.1073/pnas.0811168106.

Jenkinson, M. et al. (2012) 'FSL', Neuroimage, 62(2), pp. 782–790. doi:10.1016/j.neuroimage.2011.09.015.

Jirsa, V.K. et al. (2017) 'The Virtual Epileptic Patient: Individualized whole-brain models of epilepsy spread', Neuroimage, 145, pp. 377–388. doi:10.1016/j.neuroimage.2016.04.049.

Jülich Supercomputing Centre (2018) 'JURECA: Modular supercomputer at Jülich Supercomputing Centre', Journal of large-scale research facilities, 4, p. A132. doi:10.17815/jlsrf-4-121-1.

Jung, K. et al. (2020) 'Initial version of full-scope containerized pipeline developed', VirtualBrainCloud, ID 82642, H2020, Deliverable 3.1.

Jung, K., Eickhoff, S.B. and Popovych, O.V. (2021) 'Tractography density affects whole-brain structural architecture and resting-state dynamical modeling', NeuroImage, 237, p. 118176. doi:https://doi.org/10.1016/j.neuroimage.2021.118176.

Kringelbach, M.L. et al. (2020) 'Dynamic coupling of whole-brain neuronal and neurotransmitter systems', Proc. Natl. Acad. Sci. U. S. A., 117(17), pp. 9566–9576. doi:10.1073/pnas.1921475117.

Maier-Hein, K.H. et al. (2017) 'The challenge of mapping the human connectome based on diffusion tractography', Nat. Commun., 8(1), p. 1349.

Pijnenburg, R. et al. (2021) 'Myelo- and cytoarchitectonic microstructural and functional human cortical atlases reconstructed in common MRI space', NeuroImage, 239, p. 118274. doi:https://doi.org/10.1016/j.neuroimage.2021.118274.

Popovych, O.V. et al. (2019) 'What Can Computational Models Contribute to Neuroimaging Data Analytics?', Front. Syst. Neurosci., 12, p. 68. doi:10.3389/fnsys.2018.00068.

Popovych, O.V. et al. (2021) ‘Inter-subject and inter-parcellation variability of resting-state whole-brain dynamical modeling’, NeuroImage, 236, p. 118201. doi:10.1016/j.neuroimage.2021.118201.

Schaefer, A. et al. (2018) ‘Local-Global Parcellation of the Human Cerebral Cortex from Intrinsic Functional Connectivity MRI’, Cereb. Cortex, 28(9), pp. 3095–3114. doi:10.1093/cercor/bhx179.

Schirner, M. et al. (2015) An automated pipeline for constructing personalized virtual brains from multimodal neuroimaging data, Neuroimage, 117, pp. 343-357. doi:10.1016/j.neuroimage.2015.03.055.

Schirner, M. et al. (2021) Brain Modelling as a Service: The Virtual Brain on EBRAINS, arXiv, abs/2102.05888. doi:https://arxiv.org/abs/2102.05888.

Soares, J. et al. (2013) A hitchhiker's guide to diffusion tensor imaging, Front. Neurosci., 7, 31. doi:10.3389/fnins.2013.00031.

Tournier, J.D. et al. (2019) ‘MRtrix3: A fast, flexible and open software framework for medical image processing and visualisation’, Neuroimage, 202, p. UNSP 116137. doi:10.1016/j.neuroimage.2019.116137.

Tustison, N.J. et al. (2014) ‘Large-scale evaluation of ANTs and FreeSurfer cortical thickness measurements’, Neuroimage, 99, pp. 166–179. doi:10.1016/j.neuroimage.2014.05.044.

Zimmermann, J. et al. (2018) ‘Differentiation of Alzheimer’s disease based on local and global parameters in personalized Virtual Brain models’, NeuroImage: Clinical, 19, pp. 240–251. doi:https://doi.org/10.1016/j.nicl.2018.04.017.